Investigation of Oil Shale Response Using Terahertz-Time Domain Spectroscopy

By

Moses Eshovo Ojo*α, Patrick Mounaix* and Damien Bigourd*#

Abstract

Oil shale is an unconventional source of fuel distributed across the world with only few active explorations due to the competitive advantage price of crude oil and natural gas. However, oil shale holds important application in the context of a decline in the crude oil reserves and a spike in the oil prices. In order to prepare for the futuristic tail off in the conventional oil sources, efforts are since geared towards evaluating the oil yield potential of oil shale of different countries. In this work, a concise summary of related research in the study of oil shale analysis with particular emphasis on the Nigerian oil shale was investigated. We identified the shortcomings in the adopted techniques and suggested the complementation of a Terahertz-Time Domain Spectroscopy THz-TDS. Other than the indigenous Fischer Assay method of oil shale analysis, a combination of at least one other technique is usually incorporated in the analysis. The potential of the supplementary THz-TDS technique to yield perceptive results was addressed with promising recommendations to enhance the performance of the technique.

Keywords: Oil shale, THz-TDS, kerogen, oil yield, shale oil and oil shale-gas.

Introduction

Oil shale is a combustible source rock, composed of minerals and organic matter i.e. kerogen. The kerogen content of the oil shale are insoluble substances dispersed within the matrix of the inorganic minerals[1] [2] [3]. Oil shale is capable of generating oil and other petroleum products when subjected to pyrolytic reaction. Heating oil shale to a sufficiently high temperature causes the chemical process of pyrolysis to yield volatile vapours. The moisture content of the oil shale is firstly removed, then bitumen is formed. Bitumen is usually produced as an intermediate product during the decomposition of oil shale, with only rare exceptions. Subsequent heating of the bitumen will yield the volatile vapours which upon cooling, the shale oil will be separated from the oil shale-gas. The residue following the decomposition of the oil shale is an ash referred to as

* Université de Bordeaux, IMS UMR CNRS 5218, Bordeaux, France

α Corresponding email:moses-eshovo.ojo@u-bordeaux.fr

Corresponding email: damien.bigourd@u-bordeaux.fr

[1] R. Bouamoud, E. Moine, R. Mulongo-Masamba, A. Hamidi, M. Halim , S. Arsalane (2020) .Type I kerogen-rich oil shale from the Democratic Republic of the Congo: mineralogical description and pyrolysis kinetics. *Petroleum science*, 17, 255–267.

[2] X. Miao, M. Chen, Y. Li, H. Zhan, K. Zhao, W. Yue (2020). Simultaneous determination of organic distribution and content in oil shale by terahertz imaging. *Energy and Fuels* 34(2), 1664-1668.

[3] K. Alstadt, D. Katti, K. Katti (2012). An *in situ* FTIR step-scan photoacoustic investigation of kerogen and minerals in oil shale. *Spectrochimica Acta Part A* 89, 105– 113.

semi-coke[4 5 6 7]. Shale oil and oil shale-gas are chemically identical to the products of fossil fuel, and thus serve as a substitute for conventional crude oil and natural gas, respectively. By adopting an efficient mining technique, they could be particularly useful when the price of crude oil rises or when the hydrocarbon reserves of the fossil fuel is no longer economical for exploration[8 9 10 11].

$$\text{Kerogen} \xrightarrow{\text{pyrolysis}} \text{moisture + bitumen}$$

$$\text{Bitumen} \xrightarrow{\text{pyrolysis + cooling}} \text{oil + gas + semi-coke} \quad (1)$$

Oil shale in widespread deposits has been reported in countries such as United States of America (USA), Estonia, China, and Brazil. USA has the largest oil shale reserve in the world, with the total of 3340 billion tons. Other countries with considerable amount of oil shale reserves includes among others; China, Israel, Romania, Egypt, Nigeria, Germany, Jordan, Morocco, Turkey, and Canada[12 13 14]. The first oil shale in Nigeria, was found in Lopkanta area of Imo state, and therefore called Lopkanta oil shale. Lokpanta is geologically situated in the Lower Benue Trough of Nigeria. The Oil shale reserve of the region has been estimated as 5.76 billion tones, of which 1.70 billion barrels are recoverable[15 18]. Moreover, economic feasibility studies on the exploration of the Lokpanta oil shale has endorsed its potential to supply petroleum products even after the supposed end of crude oil supply in the year 2057[16 17]. Since the discovery of the Lokpanta oil shale, there have been only a few numbers of experimental works to quantitatively identify their oil yield

[4] Y. Ma, S. Zhou, J. Li, Y. Li, K. Chen, Y. Zhang, D. Fu (2018). Pyrolysis characteristics analysis of Chang-7 oil shale using thermal analysis and pyrolysis-gas. *Energy Exploration & Exploitation*, 36(5), 1006–1021.

[5] M. Al-Harahsheh, O. Al-Ayed, J. Robinson, S. Kingman, A. Al-Harahsheh, K. Tarawneh, A. Saeid, R. Barranco (2011). Effect of demineralization and heating rate on the pyrolysis kinetics of Jordanian oil shales. *Fuel Processing Technology*, 92, 1805–1811.

[6] W. Qing, S. Baizhong, H. Aijun, B. Jingru, L. Shaohua (2007). Pyrolysis characteristics of Huadian oil shales. *Oil Shale*, 24 (2), 147–157.

[7] P. Williams, H. Chishti (2000). Two stage pyrolysis of oil shale using a zeolite catalyst. *Journal of Analytical and Applied Pyrolysis*, 55, 217–234.

[8] . A. Akash, J. O. Jaber (2003). Characterization of shale oil as compared to crude oil and some refined petroleum products. *Energy Sources*, 25, 1171–1182.

[9] D. Fenton, H. Henning, R. Richardson (2009). The chemistry of shale oil and its refined products. *Oil Shale, Tar Sands, and Related Materials*, Chapter 21 pp 315-325.

[10] L. Zhang, X. Zhang, S. Li, Q. Wang (2012). Comprehensive utilization of oil shale and prospect analysis. *Energy Procedia*, 17, 39 – 43.

[11] Q. Yanga, Q. Yang, Y. Man, D. Zhang, H. Zhou (2020). Technoeconomic and environmental evaluation of oil shale to liquid fuels process in comparison with conventional oil refining process. *Journal of cleaner production*, 255, 120198.

[12] N. E. Altun, C. Hicyilmaz, J.Y. Hwang, A. S. Bagci, M. V. Kok (2016). Oil shales in the world and Turkey; reserves, current situation, and future prospects: A review. *Oil shale*, 23(3), 211-227.

[13] J. Bartis, T. Tourrette, L. Dixon, D. Peterson, G. Cecchine (2005). Oil shale developments in the United States; prospects and policy issues. Published by RAND cooperation, ISBN 0-8330-3848-6.

[14] J. Dyn (2006). Geology and resources of some world oil-shale deposits. *Scientific Investigations Report*, series number 2005-5294.

[15] O. Ehinola, O. Sonibare, O. Akanbi (2005). Economic evaluation, recovery techniques and environmental implications of the oil shale deposits in the Abakiliki Anticlinorium, Southeastern Nigeria. *Oil Shale*, 22(1), 5-19.

[16] L. Osuji (2015). The future of petroleum in Nigeria and prospects of shale oil as an alternative energy supplier. *J. chem. soc. Nigeria*, 40 (1), 1-4.

[17] A. Okon, D. Olagunju (2017). Economic estimation of oil shale development methods in Nigeria. *J. of Scientific and Eng. Research*, 4(9), 397-408.

potential. In this present work, we aim to present a summary of these works up till date, and thereafter propose the inclusion of Terahertz-Time Domain Spectroscopy (THz-TDS) to investigate the oil shale. This paper is mainly divided into two parts. The first part which describes the current analysis methods carried out to study the Nigeria oil shale, begins with important geochemical and biological indicators employed in the study of the oil shale – it follows by the individual techniques employed till date, and ends with a suggestive note on incorporating a supplementary technique to the already employed techniques. Part two makes a brief review of the THz-TDS as the supplementary technique in the characterization of the oil shale and concludes with a possible proposal to effectively improve the performance of the oil shale THz-TDS.

Investigation of The Nigerian Oil Shale Laboratory Techniques.

The first part of this paper begins with a preliminary study of key terminologies as applied to oil shale analysis. It highlights the commonest characterization methods employed to analyse oil shale with particular emphasis to the Nigerian oil shale.

a) Indicators of oil shale yield

Geochemical analysis is a quite common technique used to determine among others; the Total Organic Carbon (*TOC*) and Extractable Organic Matter (*EOM*) of the oil shale. The information obtainable from such analysis, are often supplemented with results from Rock Eval pyrolysis technique to determine other important oil yield parameters such as oil yield due to superficial heating S_1, maximum oil high yield due to sufficient heating S_2, pyrolytic temperature at maximum oil yield T_{max}.The kerogen content i.e. maturity type, kerogen type and kerogen quantity of the oil shale is primarily responsible for their oil yields[18]. There are indicators that have been used to evaluate the kind of the kerogen content. Below are some of them.

(i) *TOC*: This measures the percentage of organic carbon present in the oil shale. It has been established that there is a positive correlation between TOC and oil yields [18 19 20]. Mathematical relationships have been established, linking oil yield to TOC for some selected Green River oil shales in the US. Subsequent analysis of other similar Green River oil shales, and statistical treatment of the results, have produced considerably refined relationships of the form [21],

$$Oil\ wt\% = 0.8317\ X\ TOC - 0.251 \qquad (2)$$

Where, $Oil\ wt\%$ is the oil yield by percentage weight. The minimum amount of oil yield computed from the geochemical analysis of the oil shale in order to characterize them as a potential source rock, is estimated at $2.0\ wt\%$ [22].

[18] O. Sonibare, O. Ehinola, R. Egashira (2005). Thermal and geochemical characterization of Lokpanta oil shales, Nigeria. *Energy Conversion and Management*, 46, 2335–2344.
[19] C. Ekweozor, G. Un omah (1990). First discovery of oil shale in the Benue Trough, Nigeria. *Fuel*, 69(4), 502-508.
[20] L. Osuji, B. Antia (2002). An Infrared spectroscopic evaluation of the petroleum potentials of some oil shale from Lokpanta in the Lower Benue trough of Nigeria. *Journal of Applied Sciences & Environmental Management*, 6(1), 34-38.
[21] P. Williams (1983). Oil shales and their analysis. *Fuel*, 62(7), 756- 771.
[22] K. Peters, X. Xia, A.E. Pomerantz, O.C. Mullins (2016). Geochemistry applied evaluation of unconventional resources. *Evaluation and development*, Chapter 3, 71-125.

(ii) $S_1$and S_2: S_1 and S_2 evaluate the oil yield at minimal and high pyrolytic temperature respectively, in *mg/g*. While S_1 comprises of volatile hydrocarbon, S_2 consists of pyrolysable hydrocarbon[23]. A plot of either S_2 or *HI* against T_{max} have been used to determine maturity state of some other kerogen sources[24].

(iii) *HI*: *HI* represents the relative amount of hydrogen to organic carbon present in the oil shale. *HI* is inversely related to *TOC* as per

$$HI = \frac{S_2(mg/g)}{\%\,TOC}\ X\ 100 \quad (3)$$

A minimum *HI* value of $196\,mgHC/g\,TOC$ is used as an indicator of high oil yielding oil shale[24].

(iv) Kerogen type: Oil shale kerogens can be classified based on their predominant hydrocarbon constituents. The types of kerogen present in an oil shale largely controls the type of hydrocarbons generated in the oil shale. Different types of kerogen contain different amounts of hydrogen relative to their carbon and oxygen composition. Accordingly, there are four types of kerogen namely, type I, type II, type III, and type IV kerogen[25]. Type I kerogen are most likely to yield large quantities of oil and are referred to as oil prone, the type II kerogen have tendencies to yield both oil and gas and are sometimes referred to as oil & gas prone kerogen, the type III kerogen are gas prone; yielding high amount of gas, while the type IV are relatively inert under pyrolysis. A Van Krevelen diagram as shown in Fig.1 is a standard plot of Hydrogen Index (*HI*) against Oxygen Index (*OI*), commonly used to identify the kerogen type of an oil shale. The diagram has four curves which are indicatives of different kerogen type. In order to determine the kerogen type, it is customary to plot the *HI* and *OI* data of the oil shale on the Van Krevelen diagram. Fig. 1 illustrates the classification criteria of the kerogen.

(v) T_{max}: T_{max} is the maximum temperature of the oil shale pyrolytic process that corresponds to the optimum oil yield. $T_{max} > 460℃$ is the minimum temperature for efficient oil yield from an oil shale.[18]

[23] O. Faboya, O. Sonibare, J. Xu, B. Cheng, Q. Deng, Z. Wei, A. Olowookere, Z. Liao (2019). Geochemical characterisation of Lower Maastrichtian Mamu Formation kerogens, Anambra Basin, Nigeria. *Earth Environ. Sci.* 360, 012015.

[24] B. SarkiYandoka, W. Abdullah, M. Abubakar, M. Hakimi, A. Jauro, A. Adegoke (2016). Organic geochemical characterization of shallow marine Cretaceous formations from Yola Sub-basin, Northern Benue Trough, NE Nigeria. *Journal of African Earth Sciences*, 117, 235-251.

[25] H. Dembicki (2009). Three common source rock evaluation errors made by geologists during prospect or play appraisals. *AAPG Bulletin*, 93(3), 341–356.

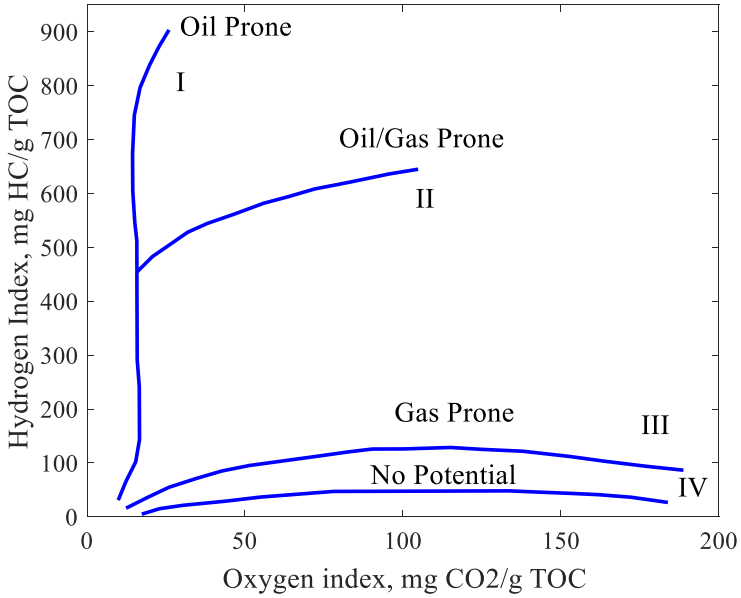

Fig.1. An example of Van-Krevelan diagram for the type I, II, III and IV kerogen.

(vi) Origin and depositional environment: Oil shale kerogen is formed millions of years ago following the decomposition of organic matter under high pressure either in the presence or absence of oxygen. The source of these organic matter (terrestrial or aquatic) and their depositional environment (anoxic, suboxic or oxic) plays important roles in determining the quality and type of kerogen in the oil shale. For example, the distribution of n-alkanes i.e. the relative fraction of short and long chain n-alkanes of an oil shale in a typical Gas chromatography plot, can be used to classify kerogen types and hence provide an idea about their origin. Moreover, the Pristane(*Pr*)/Phystine(*Ph*) ratio from the chromatography data can be used to determine the depositional environment of the organic matter. A *Pr/Ph* ratio in the range 1.0 - 3.0, indicates sub-oxic depositional conditions, while the *Pr/Ph* ratios above 3.0 and below 0.6 indicate oxidizing and anoxic conditions, respectively[26] [27] [28].

(vii) Production index (*PI*): *PI* indicates the maturity level of the oil shale. In comparison to *HI*, it is computed from Rock Eval pyrolysis. *PI* data must be interpreted with caution because they could be misleading especially when the S_1yields includes contribution from drilling additives and migrated hydrocarbons other than indigenous oils. *PI* ratio greater than 0.1 are indications of mature oil shale source rock. *PI* is related to S_1 and S_2 as per[18]

[26] W. He, Y. Sun, W. Guo, X. Shan, S. Su, S. Zheng, S. Deng ,S. Kan, X. Zhang (2019). Organic geochemical characteristics of the upper Cretaceous Qingshankou Formation oil shales in the Fuyu oilfield, Songliao Basin, China: Implications for oil-generation potential and depositional environment. *Energies* 12, 4778.

[27] M. Kok, I. Senguler, H. Hufnagel, N. Sonel (2001). Thermal and geochemical investigation of Seyitomer oil shale. *Thermochimica Acta*, 371, 111-119.

[28] G. Wang, M. Sun, S. Gao, L. Tang (2018). The origin, type and hydrocarbon generation potential of organic matter in a marine-continental transitional facies shale succession (Qaidam Basin, China). *Sci Rep*, 8, 6568.

$$PI = \frac{S_1}{S_1+S_2} \quad (4)$$

(viii) *EOM*: The directly measured quantity of bitumen, i.e. the soluble organic matter of oil shale, is referred to as *EOM*. The amount of bitumen increases with the maturity state of the oil shale. *EOM* in the oil shale can be computed from the geochemical analysis results. The minimum required *EOM* for a source rock to be classified as a potential oil source is about $500\ ppm$ [18].

(ix) Rock Eval oil yield: The Rock Eval oil yield is dependent on the S_1 and S_2 results following from the Rock Eval Pyrolysis. The Rock Eval oil yield is related to the Fischer Assay oil yield (*FAY*) as per

$$\text{Fischer Assay oil yield } (1\text{tonne}^{-1}) = 1.03(S_1 + S_2) + 7.23 \quad (5)$$

The relationship in (5) allows a direct comparison between these two quantities. A *FAY* of $42\ 1\text{tonnes}^{-1}$ is the minimum yield for economic exploration[19].

b) Adopted techniques of the Nigerian oil shale characterization

The initial field identification of potential oil shale deposits can be achieved by visual aid through simple examination of physical properties, e.g., colour, streak, specific gravity, smell etc[21]. The Nigerian oil shale which is typically dark-grey, laminated, and fissile in appearance has been found as outcrops and subcrops deposits in Lokpanta village of Imo state[19]. Several techniques have been employed to characterize the Nigerian oil shale namely: the Fischer Assay method supported by geochemical analysis, Infra-Red Spectroscopy Analysis, Gas Chromatography-Mass Spectrometer (GC-MS) and Thermal Analysis (ThermoGravimetric, TGA & Differential Thermal Analysis, DTA). As no single method is ideal[29] [30], a combination of two or more of these techniques were employed by the researchers. The Fischer Assay method involves the collection and evaluation of evolved shale oil during pyrolysis. Geochemical analysis in addition to Rock Eval-pyrolysis are often carried out to determine the indicators of the oil shale i.e. *TOC*, S_1, S_2, oil yield etc. A positive correlation between *TOC* and Fischer Assay oil yields, for example, is predominantly observed[21] [31] [32] [33] .Through the use of optics, the infra-red spectroscopy has provided a rapid means of estimating kerogen's aliphatic, aromatic, and alicyclic carbon contents, that are related to oil

[29] A. Mohammed, C. Peter, C. Alan (2012). Evaluation of several methods of extraction of oil from a Jordanian oil shale. *Fuel*, 92(1), 281-287.
[30] Z. El-Rub, J. Kujawa, E. Albarahmieh, N. Al-Rifai, F. Qaimari, S. Al-Gharabli (2019). High throughput screening and characterization methods of Jordanian oil shale as a case study. *Energies* 12, 3148.
[31] C. Gülamber, K. Ibrahim, S. Aljurf, H. Rahman (2019). Introduction of analytical methods for oil shale resource evaluation. IMCET, Antalya, Turkey, April 16 – 19.
[32] M. Barakat, E. El-Gawad, M. Gaber, M. Lotfy, A. Ghany (2019). Mineralogical and Geochemical Studies of Oil Shale Deposits in the Cretaceous/Paleogene succession at Quseir Area, Egypt. *Egyptian Journal of Petroleum*, 28, 11–19.
[33] I. Johannnes, K. Kruusement, R. Veski, J. Bojesen-Koefoed (2006). Characterisation of pyrolysis kinetics by rock-eva basic data. *Oil Shale*, 23(3), 249–257.

yields[34] [35] [36] [37]. The use of Gas chromatography-Mass Spectrometer provided fingerprint information for separating particular fractions in the kerogen; for example, the n-chain alkanes, and their subsequent identification[38] [39] [40] [41]. Another technique of importance is the thermal analysis, which involves subjecting the oil shale to increasing thermal condition. It differs from Fischer Assay Method, in that oil yield is not directly measured and no oil is collected. It studies the weight loss, kinetics of kerogen decomposition and the associated activation energy[42] [43] [44] [45]. The DTA curve of other country's kerogen has shown, that kerogen decomposition is highly exothermic in nature with high quantity of heat released which can be useful for domestic and industrial application[46] [47].

In the foremost scientific work on the Lopkanta oil shale, Chukwuemeka *et al.* collected outcrop and subsurface samples from three different locations and within 1.5 x 1.0 km belt respectively which were analysed via geochemical analysis and GC-MS analysis. The subsurface samples were retrieved from a 25.5m well at regular intervals. The average value of the estimated *FAY* of the outcrop and subcrop samples which exceeded the minimum required value was $51\ (1\text{tonne}^{-1})$ and $40.8\ (1\text{tonne}^{-1})$ respectively. The *TOC* of the outcrop and subcrop sample which were $4.6-7.4\ wt\%$ and $4.1-6.8\ wt\%$ respectively exceeded the minimum required *TOC*. The *PI* and T_{max} of both samples indicate that the oil shales are of intermediate maturity. The maturity of the subsurface samples was found to increase with depth. The *FAY* was well correlated with the geochemical results i.e. *TOC*, except for *EOM*. Regions with the lower *EOM*

[34] S. Palayangoda, Q. Nguyen (2012). An ATR-FTIR procedure for quantitative analysis of mineral constituents and kerogen in oil shale. *Oil Shale*, 29(4), 344–356.
[35] B. Chen, X. Han, X. Jiang (2016). In-situ FTIR analysis of the evolution of functional groups of oil shale during the pyrolysis. *Energy and fuels*, 30(7), 5611–5616.
[36] H. Ganz, W. Kalkreuth (1987). Application of infrared spectroscopy to the classification of kerogen types and the evaluation of source rock and oil shale potentials. *Fuel*, 66(5), 708-711
[37] M. Mroczkowska-Szerszeń, K. Ziemianin, P. Brzuszek, I. Matyasik, L. Jankowski (2015). The organic matter type in the shale rock samples assessed by FTIR-ATR analyses. *Nafta-Gaz*, 71(6), 361-369.
[38] W. Wang, S. Li, Y. Liu, D. Qiu, Y. Ma, J. Wu (2005). Analysis of the chemical constitutions of Yaojie shale oil in China by gas chromatography–mass spectrometry (GC–MS). *WIT Transactions on Ecology and The Environment*, 206, 91-100
[39] W. Blum, P. Ramstein, G. Eglinton (1990). Coupling of high temperature glass capillary columns to a Mass Spectrometer, GC/MS analysis of metalloporphyrins from Julia Creek oil shale samples. *Journal of high resolution chromatography*,13, 85-93.
[40] A. Al-Zuheri, H. Rashad, Ali Maliki, H. Hussain, N. Al-Ansari (2018). Determination of the chemical structure of the Iraqi oil shale and its hydrocarbon forms. *Engineering*, 10, 7-20.
[41] N. Ristic, M. Djokic, A. Konist , K. Geem, G. Marin (2017). Quantitative compositional analysis of Estonian shale oil using comprehensive two dimensional gas chromatography. *Fuel processing technology*, 167, 241–249
[42] A. Aboulkas, K. El-harfi, M. Nadifiyine, M. Benchanaa (2011). Pyrolysis behaviour and kinetics of Moroccan oil shale with polystyrene. *Journal of Petroleum and Gas Engineering*, 2(6), 108-117.
[43] N. Al-Ananzeh, M. L. Al-Smadi, A. Dawagreh (2018). Thermogravimetric and composition analysis of Jordanian oil shale. *Energy resources*, 40(11), 1374-1379.
[44]Z. Hua, Q. Wang, C. Jia, Q. Liu (2019). Pyrolysis kinetics of a Wangqing oil shale using thermogravimetric analysis. *Energy Science & Engineering*, 7(3), 912- 920.
[45]. M. Kok and E. Ozgur (2016). Combustion performance and kinetics of oil shales *Energy Sources*, 38(8), 1039–1047.
[46] T. Pihu, H. Arro, A. Prikk, T. Parve, J. Loosaar (2006). Combustion experience of Estonian oil shale in large power plants. International Conference on Oil Shale: "Recent Trends in Oil Shale", 7-9 November 2006, Amman, Jordan.
[47] A. Hepbasli (2004). Oil shale as an alternative energy source. *Energy, sources*, 26(2), 107-118.

corresponded to higher *FAY*, and vice versa. Their findings suggest that immature oil shale have more oil yields than mature ones. The GC-MS shows that the hydrocarbon has been composed of a mixture of type I and II kerogen, having marine algae origin. These marine algae were deposited in an anoxic condition[19].

Three years following the foremost work on the Lopkanta oil shale, a new technique was utilized to study the Lopkanta oil shale. In their work, Osuji *et. al*, subjected thirty outcrop samples to infra-red spectroscopy. The spectrum: a plot of Intensity against wavelength number (cm^{-1}), indicated absorption peaks at around $1600 - 1450\ cm^{-1}$ for a few of the samples. Absorption at this range is indicative of the presence of oil producing organic matter i.e. aromatic hydrocarbon. In addition to the spectroscopic technique, another analysis was carried out to determine the *TOC*; the outcrop samples were pulverized, and dissolved in series of chemicals, in order to extract the kerogen. The extracted kerogen was dried and weighed. By a simplified assumption, that the proportion of *EOM* is negligible, the weight of the dried kerogen was ultimately equivalent to *TOC* which measured between$0.98 - 8.75\ wt\ \%$. Based on the *TOC* values, they suggested, that the Lopkanta oil shales are mature[20].

Some years later, the research on the Lopkanta oil shale was revisited by researchers at the University of Ibadan, Nigeria. They assembled three outcrop samples labelled as LOA 21, 39 & 75 (see [18] for the labelling codes), on which thermal analysis were performed. The kinetics of the oil shale decomposition revealed a two-consecutive reaction with bitumen as an intermediate product. During the first stage of the reaction i.e. at low temperature $25 - 100$ ℃, a peak in the weight loss was recorded, corresponding to the loss of moisture. A second peak occurring at higher temperature, $300 - 570$℃ was observed in the second stage of the reaction which corresponds to the bitumen decomposition. The results from the weight loss amounted to decomposable kerogen values of $6.50 \pm 0.49,\ 4.55 \pm 0.18,\ 9.64 \pm 0.32\ wt\%$ respectively.These values generally surpassed the standard minimum decomposable kerogen of $0.5\ wt\ \%$. The results of the DTA curve and activation energy were well correlated with each other. The activation energy was maximum for the LOA 75 samples and minimum for the LOA 21 samples. Furthermore, geochemical analysis in addition to Rock Eval pyrolysis revealed the HI & T_{max} as $0.01,\ 0.01,\ 0.05$ & $427,\ 434,\ 431$ ℃ respectively, showing the immaturity state of the oil shale. The reported *TOC* were $2.13,\ 3.91,$ & $3.12\ wt\%$, and the plot of the modified Van Krevelen diagram indicated a type II kerogen content[18].

c) Compendious note on the Nigerian oil shale analysis schemes

The foregoing techniques portrayed destructive testing and seemingly unrecoverable practice of the oil shale samples. An oil shale sample subjected to a particular analysis was destroyed due to the peculiarity of the chemical and thermal nature of the techniques. In this way, a particular oil shale cannot be subject to a subsequent analysis after the previous one. Thus, different samples, though selected from the same vicinity, are required for different analysis, instead of the usage of a unique sample for all characterization. We envisage that, comparison of the different analysis results might introduce error to the interpreted data. In addition to a source of misleading results, it is noted, that the delicacy of the oil shale may have been altered via crushing, heating, chemical

treatment, and exposure to infra-red radiation[48] [49]. Due to the above two reasons we recommend the usage of an analysis that preserves the state of the sample, to be incorporated in the analysis of the Nigerian Oil shale. The Terahertz-Time domain spectroscopy (THz-TDS) is a non-destructive technique that preserves the molecular configuration of the sample after analysis; such that, the exact sample is passed on for some other sort of analysis after previously subjected to an analysis[49] [50]. As such, results from the data can be reliably deduced. In the following part, we discuss on the usage of THz-TDS to investigate the oil shale.

An Application Study of Thz-Tds in The Analysis Of Oil Shale

The last decades have experienced a tremendous generation of THz pulse both at large scale and table-top sources. The remarkable property of these pulses is attracting the attention of a wide community including industrialist and medical experts. THz pulses have enabled the study of a wide range of materials starting from cellular to non- living objects. In the framework of this paper, we limit our discussion to application of the THz pulse in the oil and gas industry. The part two of this work is sectioned to include the basic principle of THz pulse application in oil shale analysis, typical experimental setup involving oil shale characterization with THz pulse, correlation of THz experimental result with oil shale yields, and ends with viewpoints for future improvement on this technique.

a) Relevance of THz-TDS to oil shale.

THz pulses (0.1-10 THz) are electromagnetic waves, consisting of an electric and magnetic field component which vibrate sat right-angle to each other. Through interaction with a material, the electric component of the THz pulse is modified, of which the characteristics of the material are representatives of the alteration in the wave properties, thus information about the material may be deduced. This technique of material characterization is referred to as THz-TDS[51] [52] [53]. Materials such as wood, paper, fabrics, leather, plastic and rock samples are transparent in the THz frequency range, while metals and water are reflectors/absorbers of THz pulses[54]. In the case of materials that are THz-transparent, the comparison between the THz pulses transmitted through the material with respect to the incoming THz pulse can provide valuable information about the optical properties of the material.

Among its huge uses, the THz-TDS has strong applicability in the development of the oil industry, due to its non-destructive testing and strong interaction with organic matter. Conventional oil

[48] H. Zhan, Y. Wang, M. Chen, Ru Chen, K. Zhao, W. Yue (2020). An optical mechanism for detecting the whole pyrolysis process of oil shale. *Energy*, 190, 116343.

[49] Y. Li, X. Miao, H.Zhan, W. Wang, R. Bao, W. Leng, K. Zhao (2018). Evaluating oil potential in shale formations using Terahertz time domain spectroscopy. *Journal of Energy Resources Technology*, 140(3), 034501.

[50] W. Leng, H. Zhan, L. Ge, W. Wang, Y. Ma, Kun Zhao, S. Li, L. Xiao (2015). Rapidly determining the principal components of natural gas distilled from shale with terahertz spectroscopy. *Fuel*, 2015 159, 84-88.

[51] J. Haddad, B. Bousuet, L. Canioni, P. Mounaix (2013). Review in Terahertz spectral analysis, *Trends in Analytical Chemistry*, 44, 98-105.

[52] J. Guillet, B. Recur, L. Frederique, B. Bousquet, L. Canioni, I. Manek-Hönninger, P. Desbarats, P. Mounaix (2014). Review of terahertz tomography techniques. *J Infrared Milli Terahz Waves*, 35, 382–411.

[53] J. Lampin, G. Mouret, S. Dhillon, J. Mangeney (2020). THz spectroscopy for fundamental science and applications. *Photoniques*, 101, 33-38.

[54] R. Lewis (2107). Springer handbook of electronic and photonic material, Chapter 55 (Materials for THz engineering). 1339-1349.

source rocks and petroleum products have well been investigated via the THz-TDS[55 56 57 58]. Attention, though minimal, has since been attracted to oil shale mining, since its first discovery in France around the mid-eighteenth century[59]. The kerogen constituent of the oil shale is a delicate and complex heterogeneous organic substance making up a small percentage by mass of the total weight of the oil shale. The organic component of the oil shale is of most importance in the oil industry since it determines the quality, and quantity of the oil yield. The vast majority of experiments involve probing this organic content. In the generalized study of oil shales of different country, several techniques have been employed for their investigations, including the Scanning Electron Microscope (SEM)/Transmission Electron Microscope (TEM) analysis, optical spectroscopy (e.g. Nuclear magnetic Resonance NMR, Raman, Ultra-Violet UV, Fourier Transform Infra-Red FTIR, and THz spectroscopy)[26 60 61 62 63 64], as well as including those mentioned in II (b). In this part, we focus on the review of a particular type of optical spectroscopy application in the analysis of the oil shale-kerogen. Henceforth, the word 'kerogen' will be used to refer to oil shale-kerogen, except otherwise stated. The associated chemical bonds present in the kerogen Hydrocarbon (HC) absorbs selected frequency components in the optical pulse, and by analysing the optical spectrum, the relative percentage of the HC can be determined. As such, the nature of the kerogen can be deduced. In particular, the aromatic and functional groups which largely contributes to the oil yield of the oil shale, have rotational and vibrational modes within the THz frequency range. Therefore, observed THz spectra contain rich chemical information which is useful for petroleum-source analysis[49 65 66] . Moreover, the low photon energy of the THz pulse, allows a safe propagation through flammable liquids e.g. shale oil produced during the pyrolysis-THz-TDS experiment, without causing any danger of combustion[67]. Other than been able to provide abundant information on the intermolecular and intramolecular vibration modes,

[55] X. Miao, H. Zhan, K. Zhao (2017). Application of THz technology in oil and gas optics. *Science China Physics, Mechanics and Astronomy*, 60(2) 024231.

[56] R. Bao, F. Qin, R. Chen, S. Chen, H. Zhan, K. Zhao, W. Yue (2019). Optical detection of oil bearing in reservoir rock: Terahertz spectroscopy investigation. *IEE Acess*, 7, 121755- 121759.

[57] T. Lu, Z. Li, J. Bin, Z. Kun, Z. Qing, S. Lei, Z. Lin (2009). Optical property and spectroscopy studies on the selected lubricating oil in the terahertz range. *Science in China Series G: Physics, Mechanics & Astronomy*, 52(12) 1938-1943.

[58] H. Zhan, S. Wu, R. Bao, L. Ge, K. Zhao (2015). Qualitative identification of crude oils from different oil fields using terahertz time-domain spectroscopy. *Fuel*, 143, 189–193.

[59] C. Zou (2017). Unconventional Petroleum Geology, chapter 13 (oil shale), 371-387.

[60] J. Birdwell, K. Washburn (2015). Multivariate analysis relating oil shale geochemical properties to NMR relaxometry. *Energy Fuel*, 29, 2234−2243.

[61] S. Khatibi, M. Ostadhassan, D. Tuschel, T. Gentzis, H. Carvajal-Ortiz (2018). Evaluating molecular evolution of kerogen by raman spectroscopy: correlation with optical microscopy and Rock-Eval Pyrolysis. *Energies*, 11, 1406.

[62] K. Bake, A. Pomerantz (2017). Optical analysis of pyrolysis products of Green River Oil Shale. *Energy and Fuels*, 31(12), 13345–13352.

[63] Z. Zhang, H. Zhang, X. Yang, H. Jia (2016). Mineralogical characterization and washability of Longkou oil shale. *Energy Sources*, 38 (21), 3255-3261.

[64] X. Miao, M. Chen, Y. Li, H. Zhan, K. Zhao, W. Yue (2020). Simultaneous determination of organic distribution and content in oil Shale by Terahertz imaging. *Energy Fuels*, 34, 1664−1668.

[65] M. Yin, S. Tang, M. Tong (2015). The application of terahertz spectroscopy to liquid petrochemicals detection: A review. *Applied Spectroscopy Reviews*, 51(5), 379-396.

[66] H. Zhan, M. Chen, K. Zhao, Y. Li, X. Miao, H. Ye, Y. Ma, S. Hao, H. Li, W. Yue (2018). The mechanism of the terahertz spectroscopy for oil shale detection. *Energy*, 161, 46-51.

[67] F. Al-Douseri, Y. Chen, X. Zhang (2006). THz wave sensing for petroleum industrial applications. *International Journal of Infrared and Millimeter Waves*, 27(4), 481- 503.

the THz-TDS is also advantageous over other similar techniques such as the FTIR, in that, the amplitude and phase of the signal can be measured simultaneously[68].

b) Experimental setup

A typical THz-TDS setup in transmission mode, is shown in Fig. 2[69].The system consists of a laser source, optical chopper, delay stage, THz emitter [70], THz detector, two sets of parabolic mirrors (OAPMs), focusing lens (L1, L2), mirrors (M1, M2 M3 and M4) beam splitter (BS), oil shale sample and computer system. In this example, the detection scheme is made up of an Electro-Optic (EO) ZnTe crystal, wollaston prism, balanced photodiode, and lock-in-amplifier[71]. The optical and the THz beam pathways are shown in red and burgundy colours, respectively. The laser beam is split into two beams of high and low optical power by the BS; the high-power beam is used as the pump beam to generate the THz pulses, while the low-power beam is used as the probe beam to characterize the pulse. Single-cycle THz pulses generated by the THz emitter are focused by the first set of OAPMs onto the sample surfaces at normal incidence. The transmitted THz signal through the sample is collimated by the second set of the OAPMs and overlapped with the probe beam on the ZnTe. The information carried by the THz signal can be recovered by measuring its effect on the amplitude and phase of the probe beam. The QWP and Wollaston prism splits the signal into two beams and the balanced photodiode supplies the differential beam intensity to the lock-in-amplifier, where the lock-in amplifier and chopper amplifies the signal for noise free detection. By adjusting the time delay stage at a regular increasing interval, the probe beam will scan the entire length of the signal to produce a trace of the THz waveform. The measured amplitude of the THz signal is recorded on the computer at each time delay, until the full waveform of the signal is formed on the computer screen.

[68] J. Roux, F. Garet, J. Coutaz (2014). Physics and applications of terahertz radiation. Chapter 8 **(**Principles and applications of THz Time domain spectroscopy) , pp 203-231.
[69] H. Zhan, M. Chen, Y. Zhang, R. Chen, K. Zhao, W. Yue (2020). Utilization of oil shale as an electromagnetic wave absorbing material in the terahertz range. *IEEE Access*, 8, 46795-46801.
[70] J. Fülöp, S. Tzortzakis, T. Kampfrath (2020). Laser-driven strong-field terahertz sources. *Optical Mater*, 8, 1900681.
[71] M. Zhukova, E. Makarov, S. Putilin, A. Tsypkin, V. Chegnov, O. Chegnova, V. Bespalov (2017). Experimental study of THz electro-optical sampling crystals ZnSe, ZnTe and GaP. *Journal of Physics*, 917, 062021.

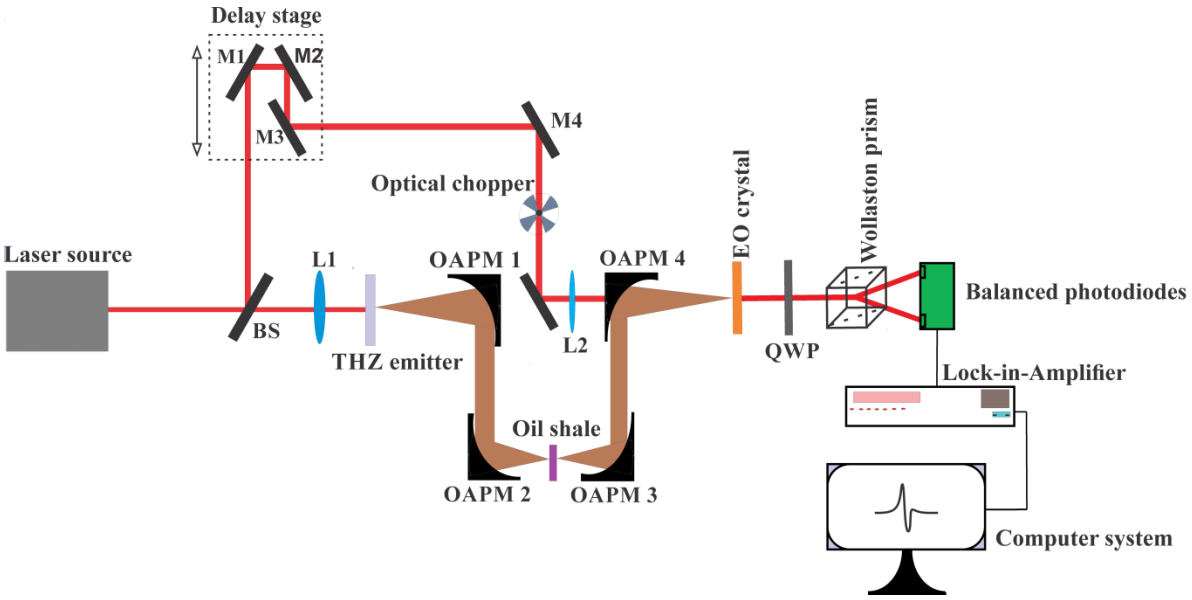

Fig. 2. A typical THz-TDS setup in the transmission mode. BS; Beam Splitter, L1-L2; Lens, M1-M4; Mirrors, OAPM1-OAPM4; Off Axis Parabolic Mirrors, QWP; Quarter Wave Plate.

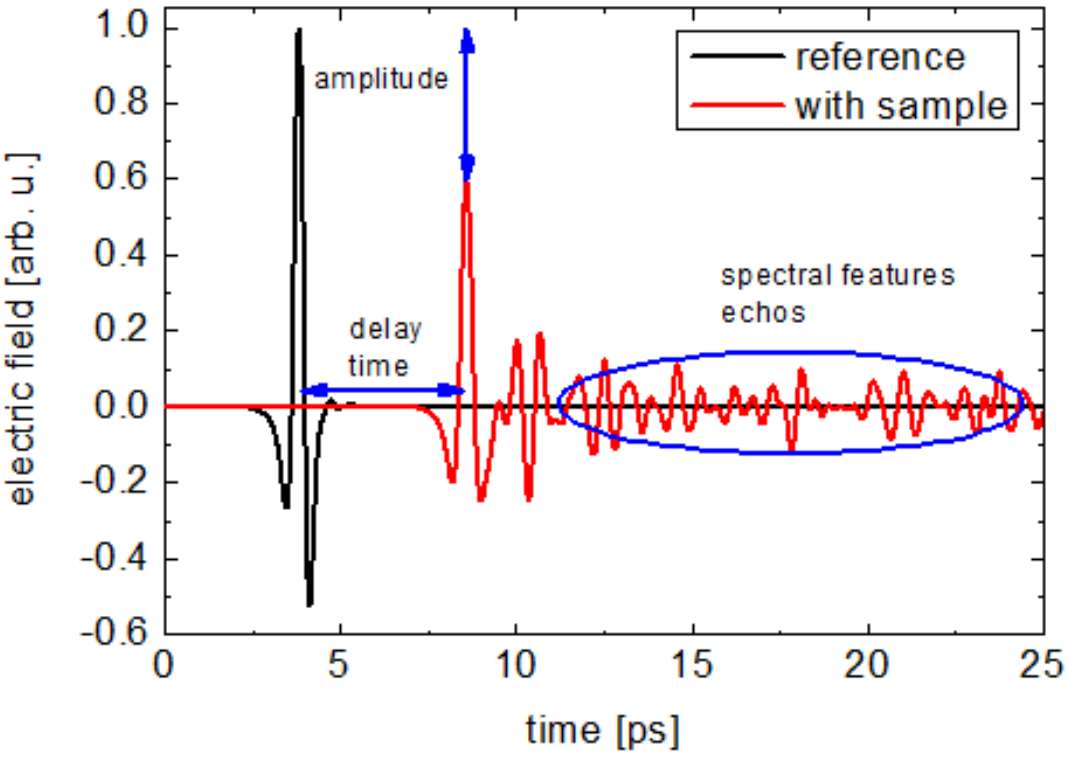

Fig. 3. The typically measured THz electric field signals. The reference (black) and sample (red) signal corresponds respectively to the detected THz pulse without and with the oil shale sample.

In order to visualize the effect of the sample on the THz pulse, the above experiment is usually performed without and with the sample. The signal obtained in the former and latter cases are respectively termed reference and sample signals. The waveform of these two signals often indicates obvious differences as shown in Fig.3. The sample signal is both delayed i.e. propagating at a lower speed and reduced in amplitude due to absorption and reflection at interfaces within the sample, as compared to the reference signal.

In practice, the signals are represented in the frequency domain in relation to each other as per [72];

$$T(\omega) = \frac{S_{sam}(\omega)}{S_{ref}(\omega)} = |T(\omega)|\, e^{-i\Delta\varphi(\omega)} \quad (6)$$

Where, ω is the THz frequencies, $\Delta\varphi(\omega)$ is the phase difference between the sample and reference signal. $|T(\omega)|$, is the transmission coefficient, and $T(\omega)$ is the complex transmittance signal. Afterwards, the $T(\omega)$ is analyzed, from which important optical properties of the oil shale can be deduced. In certain situations, the experimental setup in Fig. 2 can be adjusted in the reflection mode in order to obtain the complex reflectance signal, $R(\omega)$. In this configuration, the incoming THz pulse impinges on the sample at an inclined angle that ensures reflection. Xinyang *et al.* has utilized the reflectance configuration to generate subsurface images of the Hudian oil shale, by representing the peak amplitudes of the spectra obtained at different positions from the oil shale on a contrast image plot[64].

c) Optical properties of oil shale.

The inorganic constituent of oil shale comprises of minerals and water. Quartz, calcite, dolomite, and pyrite has been identified as been among the principal mineral constituent of oil shales[46 73 74]. During a THz-TDS at room temperature, THz pulse are mainly absorbed by the kerogen content, due to the fact, that the large macromolecules with aromatic compounds typically have vibration modes in the THz region around *0.5 – 4 THz.* When the THz-TDS is performed with a pyrolyzed oil shale sample, there are generally two major phases in the optical response of the kerogen to the THz waves. The first phase occurring at lower temperature, involves the evaporation of moisture from the oil shale thereby resulting to an increase in the strength of the transmitted THz signal. The second phase is typically characterized by a decrease in the strength of the THz pulse, due to absorption of the pulses at high temperature[49 75]. At such high temperature, the minerals are dissolved in water, then become generally conductive, and subsequently absorbing the THz pulse. Such responses are measured as the complex dielectric function of the oil shale.

$$\varepsilon(\omega) = \varepsilon_{real}(\omega) - i\varepsilon_{img}(\omega) \quad (7)$$

[72] M. Hangyo, M. Tani, T. Nagashima (2005). Terahertz Time-Domain Spectroscopy of solids:A review. *International Journal of Infrared and Millimeter Waves*, 26(12), 1661–1690.
[73] O. Sonibare, D. Jacob, C.Ward, S. Foley (2011). Mineral and trace element composition of the Lokpanta oil shales in the Lower Benue Trough, Nigeria. *Fuel*, 90(9), 2843–2849.
[74] R. Motlep, K. Kirsimae, P. Talviste, E. Puura, J. Jurgenson (2007). Mineral composition of Estonian oil shale semi-cokes sediment. *Oil Shale*, 24(3), 405–422.
[75] Y. Li, S. Wu, X. Yu, R. Bao, Z. Wu, W. Wang, H. Zhan, K. Zhao, Y. Ma, J. Wu, S. Liu, S. Li (2017). Optimization of pyrolysis efficiency based on optical property of semicoke in terahertz region. *Energy,* 126 202-207.

Where $\varepsilon(\omega)$, is the dielectric function, $\varepsilon_{real}(\omega)$ is the magnitude of THz electric field absorbed by the oil shale, $\varepsilon_{img}(\omega)$ is the scattered THz electric field [76]. The comparison between the first and second phases signifies that the absorption of THz pulse is interplay between the kerogen and the mineral constituent. At high temperature, the kerogen macromolecules decompose into lighter molecules mostly with short chains alkanes, while the minerals are decomposed into metals and metallic oxide. At this stage, the absorption of THz pulse is reversed, and mainly dominated by the metallic components[49] [77].Also, at such high temperatures, oil shale with significant pyrite composition decomposes to elemental Iron (Fe) and Sulphur (S), whose ferromagnetic response to an external magnetic field can also be studied to reveal the nature of the constituent minerals. Unfortunately, this has not been investigated in the oil shale. All information regarding the absorbed and scattered THz pulses are deduced by analysing the $T(\omega)$ signal, and subsequently retrieving the refractive index, absorption coefficient and dielectric function of the oil shale.

(i) Refractive index: The refractive index $n(\omega)$, is obtained by comparing the experimental result $T(\omega)$, with its theoretical form $T_{theo}(\omega)$ given by [68];

$$T_{theo}(\omega) = \frac{2n}{(n+1)} . \ e^{-i(n-1)\frac{\omega d}{c}} . FP \quad (8)$$

Where the first term in equation (8) is the transmission coefficient which considers the effect of amplitude decreases due to absorption as seen in Fig.2. The second term is responsible for the time delay, and represents the phase acquired by the pulse on its passage through the oil shale whose thickness and refractive index is d and n respectively. The FabryPérot (FP) term, accounts for the reflections of the pulse within the oil shale. In cases where thick oil shale is employed, FP reduces to 1, while for thin oil shale, the FP can be evaluated. Similarly, in the reflection mode, the theoretical complex reflectance signal $R_{theo}(\omega)$, is given by

$$R_{theo}(\omega) = \frac{n-1}{n+1} \quad (9)$$

Solving for $n(\omega)$, involves performing the following operations: $T(\omega) = T_{theo}(\omega)$ or $R(\omega) = R_{theo}(\omega)$. The foregoing equation is an inverse value problem that can be solved analytically by assuming an initial guess solution. The fixed-point iteration, Newton Raphson and Nicolson-Ross-Weir method have been so far used to obtain $n(\omega)$ which has been shown to exhibit good correlation with oil yield of oil shales[78] . A plot of $n(\omega)$ normally indicates a narrow decrease with ω. In general, oil shales with lower $n(\omega)$, exhibits a negative correlation with oil yields, i.e. high-oil yielding oil shales have lower $n(\omega)$ and vice versa[72] [79] [80]. It is worth mentioning that the experimental techniques employed in preparing the samples, have impact on the

[76] R. Jesch, R. Mclaughlin (1984). Dielectric measurements of oil shale as functions of temperature and frequency. *IEEE Transactions on Geoscience and Remote Sensing, 22(2), 99-105.*

[77] Y. Mai and S. Li (2018). The mechanism and kinetics of oil shale pyrolysis at the presence of water. *Carbon Resources Conversion* , 1(2), 160-164.

[78] T. Ozturk, M.Güneşer (2018). Electrical and electronics properties of materials, chapter 5 (Measurement, methods, and extraction techniques to obtain the dielectric properties of materials).

[79] Y. Li, X. Miao, H. Zhan, W. Wang, R. Bao, W. Leng, Kun Zhao (2018). Evaluating oil potential in shale formations using terahertz time domain spectroscopy. *Journal of Energy Resources Technology*, 140(3).

[80] X. Miao, H. Zhan, K. Zhao, Y. Li, Q. Sun, R. Bao (2016). Oil yield characterization by anisotropy in optical parameters of the oil shale. *Energy and Fuels*, 30(12), 10365–10370.

outcome of the measured $n(\omega)$. Yizhang *et al.* observed that using pulverized over bulk oil shale samples possessed no true correlation with the oil yield. Due to the complex heterogeneity of the oil shale, their properties were altered upon mechanical processing[79] .Thus; it is usually preferable to work with the bulk samples, in which case the original form is preserved. Oil shale has shown to possess anisotropy, in which their optical properties differ in different plane. The presence of lamination, i.e. alternating layers with varying organic matter content in oil shale is a possible reason for anisotropy. As such, during field extraction, it is recommended to cut through the earth crust at specific plane, preferably at the bedding plane of deposition. Xinyang *et al.* [80] investigated the anisotropy of some oil shale in relation to oil yield. In their procedure, they used oil shales cut at a direction parallel to the bedding plane. The refractive index was measured when the incoming THz pulse was incident parallel to the bedding plane of the oil shale, to obtain n_0, then the oil shale is rotated up to 90º to obtain the minimum refractive index, n_{90}. They observed a symmetric behaviour in $n(\omega)$ at every 180º. The anisotropy in $n(\omega)$ is given by

$$\Delta n(\omega) = n_0(\omega) - n_{90}(\omega) \quad (10)$$

A strong positive correlation between $\Delta n(\omega)$ and oil yields from different oil shale has been observed[80] .

(ii) Absorption coefficient: The absorption coefficient $\alpha(cm^{-1})$, measures the magnitude of absorbed THz pulse. $\alpha(\omega)$ is proportional to the imaginary component of the complex refractive index [68],

$$\alpha(cm^{-1}) = \frac{2\omega}{c}\mathrm{Im}[n(\omega)] \quad (11)$$

Typically, $\alpha(cm^{-1})$ increases with THz frequency and falls between *400-1800 cm^{-1}*. A comparison between the absorption plots from different oil shales analysis has indicated that, higher $\alpha\ (cm^{-1})$ corresponds to higher oil yield, and vice versa. However, when the complex refractive index in equation (11) is replaced by $\Delta n(\omega)$, the value of the new absorption coefficient $\Delta\alpha\ (cm^{-1})$, will be lower for higher oil yields, and vice versa[69] [80] [81]. In order to reveal detailed information about the bulk samples of the Hudian oil shale, Yi *et al.* [75] made several absorption plots at different pyrolysis temperature, to determine the T_{max} for useful oil yields. The T_{max} value corresponded to the maximum recorded temperature just before inconsistency in the absorption plot begins to appear; possibly due to THz absorption by metallic oxides in the pyrolyzed oil shale.

(iii) Dielectric function: The relationship between n, ε and magnetic permeability μ, (wher e μ is a measure of the magnetic response of the oil shale to the THz pulse) is given by, $n = \sqrt{\varepsilon.\mu}$. As in most oil shale THz-TDS, the magnetic permeability is ignored, so that[79],

$$n^2 = \varepsilon \quad (12)$$

[81] B. Rima, L. Zhang, Z. Lei, Z. Kun, W. Wei, M. Yue, W. Xun, L. Hua, L. Yuan, X. Zhi (2015). Probing the oil content in oil shale with terahertz spectroscopy. *Science China Physics Mechanics and Astronomy*, 58(11), 114211.

A closely related parameter to the dielectric function is the conductivity σ. The solution of Maxwell equation shows a linear proportionality between ε and σ. Following the work of Y *et al.* [82] which have demonstrated a strong relationship between the ε (and σ) with respect to pyrite and water concentration of simulated anisotropic rock samples, there might exist a likelihood of such relationship in the oil shale.

d) Oil shale-THz waveform (spectrum) characteristics

THz-TDS is rather a comparative than a quantitative study. It serves as an important supplementary technique, to validate the findings from other techniques. The shape and the corresponding spectrum, as well as the maximum amplitude of the THz pulse upon transmission through the oil shale are among the most relevantly studied parameters, used for a qualitative evaluation of the oil shale properties.

(i) Waveform profile: The THz profile of different oil shales obtained at ambient condition i.e. room temperature can be clearly distinguished by the distinct time delay and maximum electric peak E_p, of their waveforms. The minimum peak amidst other peaks has been identified as high-oil yield oil shale, and vice versa. [69] [72] Moreover, investigation has been carried out, on the waveform of a single oil shale under increasing temperature up to 1000 ℃, and a different trend was observed. The plot of E_p of the waveform obtained at each pyrolysis temperature made by Honglei *et al.* [49], has revealed four stages of oil shale decomposition; from $25-200$ ℃, E_p increased, then stabilized around $200-300$ ℃, followed by a gradually increase from $300-500$ ℃ until a maximum is reached, then a sharp decrease between $500-600$ ℃ was observed. During the first stage, the initial increase in $E_p$was due to moisture loss and become stabilized during the second stage after the moisture content was at minimum. During the third stage, the macromolecules of the kerogen were broken down, resulting to an unexpected increase in E_p possibly due to the loss of more moisture. During the fourth stage, THz pulses were absorbed due to the decomposition of the minerals to their respective metallic oxides resulting to decrease in E_p nearly up to the same magnitude at 25℃. In a recent work, Honglei *et.al* [69]investigated the absorptive behaviour of oil shales at temperature beyond 600 ℃, and observed that, the E_p at 1000℃, was much lesser than at 25℃, due to metallic (semi-coke) formation.

(ii) Spectrum plot: The Fourier transform of the sample THz pulse shown in Fig 3, generates the corresponding spectrum given in Fig. 4. A typical plot of an oil shale-THz spectrum and its reference spectrum are differentiable based on amplitude differences. Obvious absorption dips which could have been a good indicator of the presence of organic compounds have not been well observed in the THz spectrum of oil shale for the range of frequencies less than 2THz[79] .

[82] Y. Wang, J. Chen, S. Althaus, M. Yu, J. Chen (2019). Electrical properties of unconventional source rocks from micro-CT using numerical mixing law. *Fuel*, 254, 115576.

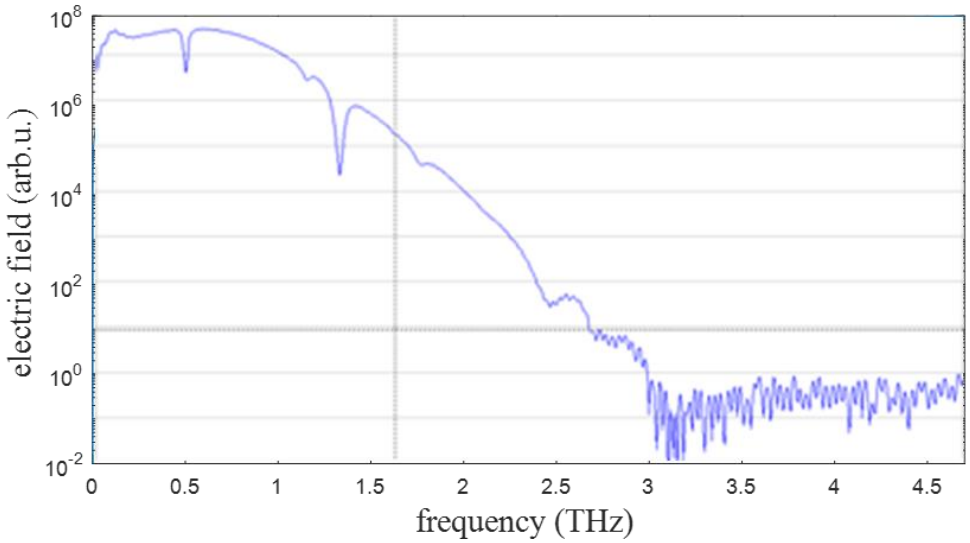

Fig. 4. A Typical spectrum plot from a THz-TDS

(iii) Amplitude measurement: THz subsurface imaging of oil shales has been achieved via the reflection mode of the THz-TDS[72]. The reflected THz amplitude from different regions of the oil shale was employed to reconstruct the non-uniform distribution of organics on the oil shale surface. Three regions corresponding to high kerogen, low kerogen and mineral regions were observed based on the intensity distribution. Results from optical micrographs and micro-Raman spectra showed good agreement with the THz contrast image .

Conclusion and Outlook

Source rocks in the Lopkanta area of Nigeria have been identified as oil shales, following the satisfaction of the requirements for such classification. Majority of the analysed samples were outcrops, whose results (from different analysis techniques) were validated against the geochemical characteristics of the oil shale. Some of the characteristics yielded the expected correlation. Generally, the oil shales were classified as been type I & II with immature to intermediate maturity level. Due to destructive nature of the techniques employed, we suggested the usage of an optical spectroscopic technique based on THz pulse irradiation. Following this suggestion, we presented a general and concise review work involving the application of THz-TDS to oil shale analysis. Single-cycle THz pulses were employed to probe the oil shale in order to determine the relative amount of oil yields, determine the maximum temperature for efficient oil yield, and generate contrast images of the oil shale constituent. Since in the past few years, there has been a growing trend in the use of THz-TDS to investigate the oil shale, we are quite hopeful that adoption of some techniques would guarantee additional information about the oil shale. As such, we make the following suggestion; firstly, we propose the adoption of a THz-Time Resolved Spectroscopy (THz-TRS) technique[83] to solve the unresolved absence of absorption peaks in the THz spectrum of the oil shale. THz-TRS are transient absorption techniques in which

[83] Q. Zhou, X. Zhang (2011). Applications of time-resolved terahertz spectroscopy in ultrafast carrier dynamics (Invited Paper). *Chinese Optics Letter*, 9(11) 11000.

changes in the THz spectrum are monitored after the samples are photo-excited. The fluorescence, resulting from the decay to a lower state is probed by short THz pulses to reveal quantum behaviours such as electronic transition, vibration, rotational modes etc. Secondly, the presence of ferromagnetic elements in the oil shale can be investigated assuming that the oil shale is exposed to an external magnetic field [84] in which the measured magneto-optical effect may reveal the nature of the minerals present. Lastly, the geological evolution of the kerogen can be studied by adopting a THz-based evolutionary kinetic study utilized by Rima *et al.* [85] [86] to investigate a different kerogen-source. The evolutionary trend would provide useful information to the geologist about the type and organic origin (marine algae or terrestrial plants) of the kerogen.

Acknowledgement
This work has been supported by the Petroleum Technology Development Fund (PTDF) Overseas Scholarship Scheme.

[84] S. Chen, F. Fan, S. Chang, Y. Miao, M. Chen, J. Li, X. Wang, L. Lin (2014). Tunable optical and magneto-optical properties of ferrofluid in the terahertz regime. *Optics Express*, 22(6), 6313.
[85] R. Bao, X. Luan, S. Wu, X. Yu, L. Zheng (2018). Detecting marine kerogen from Western Canada Basin using Terahertz Spectroscopy. *ACS Omega*, 3, 7798−7802.
[86] R. Bao, S. Wu, K. Zhao, L. Zheng, C. Xu (2013). Applying terahertz time-domain spectroscopy to probe the evolution of kerogen in close pyrolysis systems. *Science China Physics, Mechanics and Astronomy*, 56, 1603.